# Pump Characteristic Based Optimization of a Direct Water Cooling System for a 10kW/500kHz Vienna Rectifier

Uwe DROFENIK, Gerold LAIMER and Johann W. KOLAR
Power Electronic Systems Laboratory, ETH Zurich
ETH-Zentrum / ETL H12, CH-8092 Zurich, Switzerland
Phone: +41-1-632-4267, Fax: +41-1-632-1212, E-mail: drofenik@lem.ee.ethz.ch

***Abstract –*** A high power density 10kW/500kHz three-phase PWM rectifier (Vienna Rectifier) is under development. Due to preliminary measurements and numerical simulations the total efficiency is assumed to be 95% at full load, resulting in power losses of up to 150W in each multi-chip power module realizing a bridge leg of the rectifier. In order to keep the power density of the system high direct water cooling is employed where water is in direct contact with the module base plate. Based on the measured characteristic of the water pump (pressure drop dependent on water flow) the geometry of different water channel structures below the module base plate is systematically optimized based on analytical expressions which are formulated based on the well-established theory of fluid dynamics. The design optimization is constrained by the desire to keep the geometry of the water channels in a range that allows simple and low-cost manufacturing. The aim is to find a channel structure resulting in a minimum thermal resistance of the power module for a given pump characteristic.

In this paper a very simple slot channel is investigated. The dependency of the thermal resistance on the cooling system is calculated in dependency on the height of the slot channel, and an optimized channel height is found under the side condition of simple manufacturability. Discussing the shortcomings of the simple slot structure, a novel metallic inlay structure is introduced and optimized resulting in a reduction of the thermal resistance of the direct water cooling scheme as compared to the slot channel system. All theoretical considerations are verified via experimental measurements. The general optimization scheme introduced in this paper can easily be adapted to other cooling problems.

## I. INTRODUCTION

A 10kW Vienna Rectifier [1] is under development where each bridge leg is realized by a multi-chip power module employing CoolMOS switches and SiC schottky diodes which facilitate switching frequencies of up to *500kHz* in hard-switching mode. Based on first measurements and simulations the total system efficiency is approximately *95%* and/or the power loss of each module is about *150W*. Due to the high switching frequency the inductive components can be realized in compact and light-weight form. Therefore, the volume of the heat sink and cooling system takes significant impact on the total rectifier power density $[kW/dm^3]$.

Water cooling is highly efficient in removing large quantities of heat and requires only little space compared to conventional forced air cooling. For mounting the module on metal heat sink thermal grease is used for eliminating thin air layers which would cause thermal isolation. However, thermal grease still shows a significant thermal resistance which is often not exactly known. Therefore, direct water cooling, where the water is in direct contact with the power module base plate is considered which also allows avoiding large metal heat sinks. Metal heat sinks would increase the system weight and could cause increased common mode EMI for high switching frequencies.

In this paper simple slot channel geometry is compared to an advanced mini-channel scheme under on the following conditions:

- Both cooling schemes are driven by pumps of equal characteristics. This definition is an important side condition for the considerations in this paper.
- Both cooling schemes are limited to the same overall dimensions.
- Both schemes are optimized concerning minimum thermal resistance between water temperature and power module base plate.
- Manufacturing of the geometry should be possible in a simple and low cost way. This means that micro-channel structures with channel diameters of only a few $100\mu m$ are not considered.
- The comparison is based on analytical equations and verified via numerical simulations and experimental measurement, i.e. the optimization procedure is systematic and not on a try-and-error basis.

## II. SIMPLE SLOT CHANNEL

### *2.1 Pump Characteristic and Slot Channel Geometry*

The pump is generally described by a characteristic showing the pressure drop $\Delta p_{PUMP}$ $[N/m^2]$ in dependency on the flow rate $\dot{v}$ $[m^3/s]$ of the water. A heat exchanger and pipes carrying the water contribute to additional pressure drop in the cooling system. Therefore, the pressure drop $\Delta p_{12}$ $[N/m^2]$ is measured directly across a valve which will be replaced by the heat sink later (cf. **Figs.1**(a) and (b)). The pressure drop $\Delta p_{12}$ $[N/m^2]$ is used as basis for all calculations in the following and is approximated by a second order polynomial (dimension of $\dot{v}$ is $[m^3/s]$) as

$$\begin{aligned}\Delta p_{12} &= \Delta p_{12}(\dot{v}) = p_1 - p_2 = \\ &= 14.7\cdot 10^3 - 148.3\cdot 10^6\,(\dot{v}) - 13.88\cdot 10^{12}\,(\dot{v})^2\end{aligned} \tag{1}$$

Finding the characteristic (1) for a given cooling system is done experimentally by replacing the heat sink with a simple valve and measuring pressure drop and flow rate for different valve-settings. We want to point out that this measured characteristic can be very different from the pump characteristic given by the manufacturer.

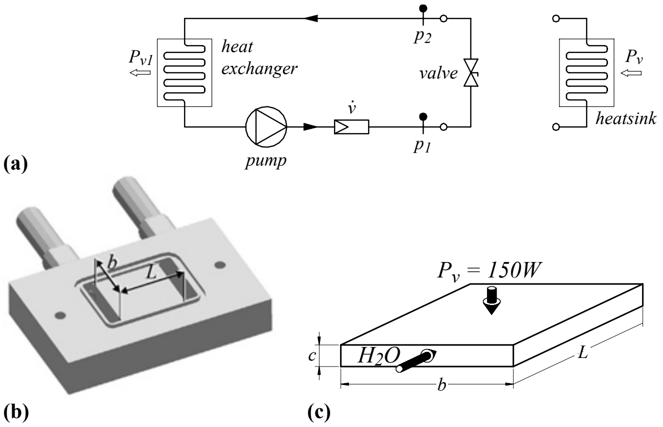


**Fig.1: (a)** Cooling system employing pump, heat exchanger and pipes. The valve is used to control the water flow while measuring the according pressure drop $\Delta p_{12}= p_1 - p_2$ for determining the characteristic of the water cooling system (cf. (1)). After the characteristic has been determined the valve is replaced by the heat sink. **(b)** The heat sink is made from plastic (characterized by $\lambda_{th}$ *=0.25 W/(Km)*). The base plate of the power module (not shown) sitting on top of the heat sink is covering the rectangular area $A_{BasePlate} = b \cdot L$ resulting in direct contact of the water with the base plate ("direct water cooling"). **(c)** Geometry of the slot channel carrying the water (*L=20mm*, *b=19.2mm*). Heat flow $P_V$*=150W* is impressed from the base plate of the power module.

## *2.2 Calculation of Water Flow and Pressure Drop in a Slot Channel*

Laminar water flow through a channel (*c<< b)* results in a pressure drop (correction factor for slot channels as described in (6.91), (6.92) in [2.1] plus equation given in (3.221) in [3])

$$\Delta p_{SlotChannel,lam}(\dot{v}) = \frac{48\,\rho\,\nu\,L}{(bc)\,d_h^2}\;\dot{v} \tag{2}$$

with the hydrodynamic diameter $d_h$*=2bc/(b+c)*, water flow $\dot{v}$ *[m³/s]*, water density $\rho = \rho_{H20} = 992\ kg/m^3$, cinematic viscosity $\nu = \nu_{H20,40°C} = 658 \cdot 10^{-9}\ m^2/s$, and the slot channel geometry *L=20mm, b=19.2mm*, where *c* is the *optimization parameter* (Fig.1(c)). For turbulent water flow the pressure drop in the same slot channel is determined by ((3.261) in [3])

$$\Delta p_{SlotChannel,turb}(\dot{v}) = \frac{L\frac{b+c}{2bc}\rho\frac{1}{2}(\frac{\dot{v}}{bc})^2}{(0.79 \cdot \ln(\frac{2\dot{v}}{(b+c)\nu}) - 1.64)^2} \tag{3}$$

For determining if the water flow is laminar or turbulent one has to calculate the Reynolds number

$$\mathrm{Re}_{Channel} = \frac{w_m \cdot d_h}{\nu} = \frac{2\dot{v}}{(b+c)\nu} \tag{4}$$

of the problem (page 351 in [3]) with the average flow velocity

$$w_m = \dot{v} / A_q = \dot{v} / (bc) \tag{5}$$

For $Re_{Channel} < 2300$ the problem is laminar ((7.1) in [2.1]), turbulent otherwise. Assuming the problem as turbulent the water flow $\dot{v}$ for a given geometry (*L, b, c*) of the slot channel can be calculated using (1) and (3). Based on $\dot{v}$ one can then calculate the Reynolds number employing (4). If the Reynolds number is higher than *2300* the assumption is justified, otherwise the water flow $\dot{v}$ and the Reynolds number have to be calculated using (1) and (2). This mathematical procedure is shown in **Fig.2** for different values of channel height *c*.

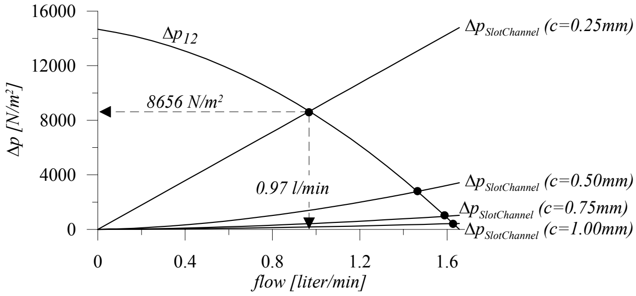


**Fig.2:** Characteristic $\Delta p_{12}(\dot{v})$ and heat sink characteristic $\Delta p_{SlotChannel}(\dot{v})$ defining the actual water flow $\dot{v}$ and the pressure drop $\Delta p$ *[N/m²]* for the selected slot channel geometry (*L=20mm, b=19.2mm*). Note that the water flow $\dot{v}$ is given in all diagrams in *[liter/min]* while all calculations including (1) are performed in SI-units *[m³/s]*.

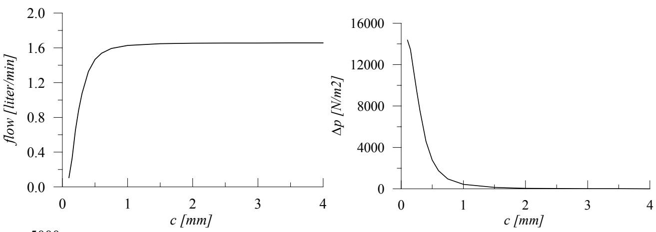


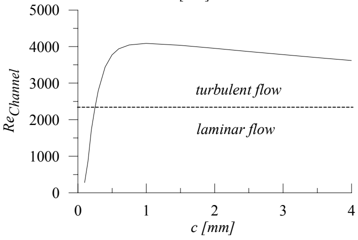


**Fig.3:** Water flow, pressure drop (cf. Fig.2) and Reynolds number indicating laminar or turbulent flow in dependency of the slot channel geometry (height *c*).

Water flow, pressure drop and $Re_{Channel}$ are shown in **Fig.3** in dependency on the height *c* of the slot channel (see Fig.1(c) for geometry-definitions). For small height *c* the pressure drop across the heat sink increases significantly and the water flow is reduced accordingly. Only for very small channel heights ($c<250\mu m$) the flow is laminar.

## *2.3 Calculation and Minimization of the Thermal Resistance of the Slot Channel Geometry*

Since the heat sink has to guide the water flow but does not have to conduct heat it can be made of plastic. The heat flow is directly from one wall, i.e. the power module base plate into the water. Therefore, the thermal model for water flow along a hot plate has to be applied. With the average flow velocity $w_m$ already calculated in (5), this type of thermal problem comes with a different definition (page 324 in [3]) of the Reynolds number

$$\mathrm{Re}_{AlongPlate} = \frac{w_m \cdot L}{\nu}\ . \tag{6}$$

For calculating the thermal resistance we first have to define the Nusselt number $Nu_{AlongPlate}$ which is defined for this type of problem (valid for both laminar and turbulent flow as given in equations (3.196), (3.207), (3.208) in [3]) as

$$Nu^2_{AlongPlate} = \left[ \frac{2 \cdot \frac{\sqrt{\pi}}{2} \mathrm{Re}^{1/2}_{AlongPlate} \mathrm{Pr}^{1/2}}{(1 + 2.09 \cdot \mathrm{Pr}^{1/4} + 48.74 \cdot \mathrm{Pr})^{1/6}} \right]^2 + \left[ \frac{0.037 \cdot \mathrm{Re}^{0.8}_{AlongPlate} \mathrm{Pr}}{1 + 2.443 \cdot \mathrm{Re}^{-0.1}_{AlongPlate} (\mathrm{Pr}^{2/3} - 1)} \right]^2 \tag{7}$$

The Prandtl number $Pr$ in (7) is a fluid parameter, for water we have $Pr = Pr_{H20,40°C} = 4.328$. Based on $Nu_{AlongPlate}$ one can calculate the thermal resistance $R_{th,aboveSlot}$ between the water ($T_a = T_{H20,ambient} = 40°C$, $\lambda_{H20} = 0.63\ W/(Km)$) and base plate above the slot channel as ((1.47) and (1.77) in [3])

$$R_{th,aboveSlot} = \frac{L}{Nu_{AlongPlate}\ \lambda_{H20}\ A_{BasePlate}} = \frac{1}{Nu_{AlongPlate}\ \lambda_{H20}\ b} \tag{8}$$

As shown in **Fig.4** the minimum thermal resistance $R_{th,MIN} = 0.1 K/W$ is given for $c = 300 \mu m$. This is in accordance with the theory of micro-channels for single-phase liquid cooling systems ([4]).

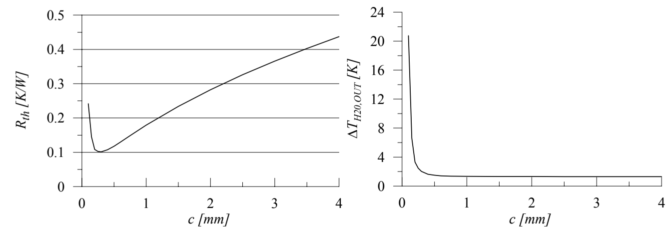


**(a)** **(b)**

**Fig.4:** **(a)** Thermal resistance between power module base plate above slot channel (area $L \cdot b$) and cooling water dependent on the channel height $c$ (cf. Fig.1(c)). **(b)** Difference $\Delta T$ of water temperature between entrance and end of the slot channel. For narrow channels (small values of $c$) $\Delta T$ increases as the water flow reduces (Fig.3(a)), resulting in a sharp increase of the thermal resistance.

### *2.4 Influence of the Pipe Structure between Water Inlet/Outlet of the Heat Sink and the Slot Channel*

#### *2.4.1 Additional Pressure Drop*

In the previous sections (2.2) and (2.3) the thermal resistance between base plate and water in the slot channel has been discussed resulting in Fig.4(a). The influence of the pipe structure inside the heat sink guiding the water between inlet/outlet and slot channel has been neglected. The pipe structure influences all calculations due to an additional internal pressure drop and additional heat transfer between base plate and water across inflow area and outflow area where the slot channel geometry cannot be applied. **Figure 5** shows a detailed geometry of the three-dimensional pipe structure.

Analytical equations describing the pressure drop in all kinds of pipes of circular and non-circular cross-sections along different kinds of bends are given in the literature in the very general form (based on experiments)

$$\Delta p = \xi \cdot \tfrac{\rho}{2} w_m^2 , \tag{9}$$

with values of the coefficient $\zeta$ given in tables (page B52 in [4.2]). A straightforward calculation of the total pressure drop in the pipe structure defines all relevant values of $\zeta$ along the water flow path shown by the solid line in Fig.5. The according flow velocities $w_m$ are given by the quotient of water flow rate $\dot{v}$ and actual cross sectional area $A_q$. Adding all individual pressure drops result in a total pressure drop of the given pipe structure $\Delta p_{PipeStructure}$. In consideration of the fact that pipe bends show a significant contribution to pressure drop the locations of large pressure drops are highlighted in gray and labeled as (1)…(5) in Fig.5. Unfortunately, the $\zeta$-values of bends vary by a factor of $8$ according to the exact definition of pipe and bend. For the complex three-dimensional flow pattern within the pipe structure it is, therefore, not possible to accurately calculate the pressure drop $\Delta p_{PipeStructure}$ without any experimental measurement or numerical CFD-simulation.

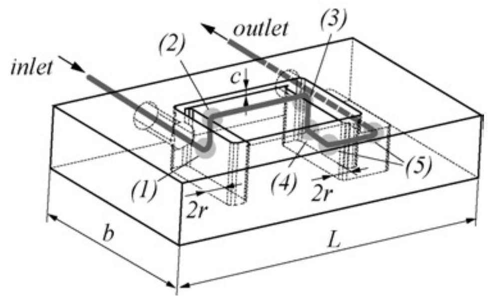


**Fig.5:** Geometry of the three-dimensional pipe structure inside the heat sink guiding the water flow along inlet → inflow area → slot channel (height $c$) → outflow area → outlet. The gray shaded regions labeled (1), (2), (3), (4), (5) indicate significant pressure drop within the pipe structure.

We can write in a very general form

$$\Delta p_{PipeStructure} = \sum_{i=1..5} \xi_{(i)} \cdot \tfrac{\rho}{2} w^2_{m,(i)} = \tfrac{\rho}{2} \dot{v}^2 \sum_{i=1..5} \frac{\xi_{(i)}}{A^2_{q,(i)}} . \tag{10}$$

Only the water flow cross sectional areas $A_{q,(2)}$ and $A_{q,(3)}$ are proportional to the slot channel cross sectional area $A_{q,SlotChannel} = b \cdot c$. Therefore, (10) can be written as

$$\Delta p_{PipeStructure} = (x_a + \frac{x_b}{A^2_{q,SlotChannel}})\ \dot{v}^2 \ . \tag{11}$$

The parameters $x_a$ and $x_b$ are to be defined from experimental measurement. This means that two heat sinks with different slot channel height $c$ have to be manufactured and the corresponding flow rate $\dot{v}$ and pressure drop $\Delta p_{12}$ have to be measured. Equations (2) and (3) have to be modified as

$$\Delta p_{12,lam}(\dot{v}) = \Delta p_{SlotChannel,lam}(\dot{v}) + (x_a + \frac{x_b}{A^2_{q,SlotChannel}})\ \dot{v}^2 \tag{12}$$

$$\Delta p_{12,turb}(\dot{v}) = \Delta p_{SlotChannel,turb}(\dot{v}) + (x_a + \frac{x_b}{A^2_{q,SlotChannel}})\ \dot{v}^2 \tag{13}$$

Inserting the two measured flow rates and pressure drops plus the according value of $c$ in (12) and (13), and defining the flow type dependent on the Reynolds-number ((4) and (5)) gives two equations for $x_a$ and $x_b$. For two different slot channel heat sinks with $c = 0.35mm$ and $c = 2.5mm$ we received $x_a=8.3e12$ and $x_b=130$. This is valid for all channel geometries discussed in this paper because the pipe structure does never change.

### 2.4.2 Thermal Resistance of Inflow/Outflow Area

Due to the heat flow from the base plate into the water also inflow area and outflow area contribute to the thermal resistances $R_{th,IN}$ and $R_{th,OUT}$ that are connected in parallel to the thermal resistance of the channel (Fig.4). Water flow in these two areas is quite complex to describe analytically and specific for this problem so that according models are not available in the literature. Based on numerical CFD-simulations we found in good approximation $R_{th,flowArea}= R_{th,IN} \parallel R_{th,OUT} = 0.4K/W$ for $c>1.2mm$ and $R_{th,flowArea}= R_{th,IN} \parallel R_{th,OUT} = 1.0K/W$ otherwise. This rough approximation is justified because the thermal resistance of the channel area around the minimum is significantly smaller than $R_{th,flowArea}$. The definition of $R_{th,flowArea}$ is not dependent on the channel geometry and can, therefore, be employed for all cooling schemes as discussed in this paper.

## 2.5 Experimental Results

The experimental setup as shown in Fig.1(a) consists of a pump (Eheim 1048), a heat exchanger, and pipes with a circular cross sectional area and an inner diameter of 8mm. The heat sink is manufactured from PEEK™ polymer material which is convenient for rapidly producing prototypes by cutting and milling. For mass production one would, for example, employ POCAN™ (polybutylene terephthalate and polyethylene terephthalate) which can be manufactured in a cost-efficient way by injection molding. Heat sinks with slot channel heights *c= 0.2mm, 0.35mm, 0.75mm, 1.5mm, 2.5mm* have be manufactured. The power module was replaced by a heat source made by a block of copper with heating resistors placed on top. This heat source is thermally isolated so that all heat flows directly from the heating resistors through the copper block to the water surface (**Fig.6**). The copper block acts as a heat spreader creating equally distributed thermal power flow

$$\dot{q} = \frac{P_V}{A_{BasePlate}} = \frac{150W}{25 \cdot 34mm^2} = 17.6\frac{W}{cm^2} \quad (14)$$

into the water. The "base-plate" temperature is measured by thermocouples put into two holes (*2mm* diameter) drilled into the copper block. Since thermal conductivity of copper is not infinite, there is a small temperature gradient along the base plate of $\Delta T<4°C$ for $c<2.5mm$. For calculating the thermal resistance of the cooling system the average temperature value from the two measured temperatures is formed. The ambient temperature of the cooling water is *30°C*.

The measured results depict in **Figure 7** show a good match with the theory (solid lines, considering (12), (13), (section 2.4.2)). The dashed lines show the theory neglecting the influence of the internal pipe structure of the heat sink (see sections (2.2) and (2.3)). Only in close vicinity of the minimum of the thermal resistance $R_{th}$ (**Fig.4**) the additional parallel thermal resistance $R_{th,flowArea}$ can be neglected.

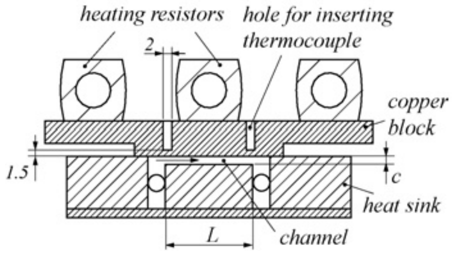


**Fig.6:** Thermally isolated copper block with heating resistors and thermocouples replacing power module and heat sink and providing equally distributed thermal power flow of *17.6W/cm²*.

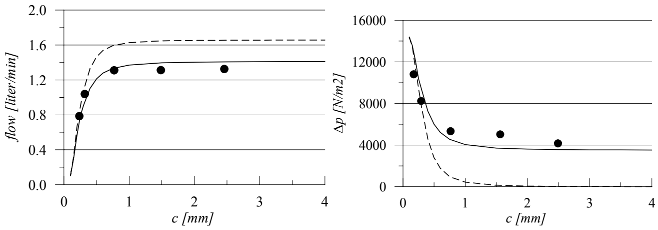


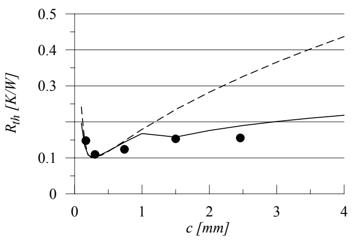


**Fig.7:** Neglecting the influence of the pipe structure inside the heat sink results in the characteristics shown in dashed lines (already shown in Fig.3 and Fig.4(a)). Performing the calculations as described in section (2.4) gives the curves shown by solid lines. The black dots are results of experimental measurements.

# III. IMPROVING THE SIMPLE SLOT CHANNEL BY A NOVEL METAL INLAY CONCEPT

## 3.1 Metal Inlay Concept

The main idea of the slot channel described in the previous chapter is to bring the power module base plate in direct contact with the water in order to avoid thermal resistances introduced by a thermal grease layer between base plate and a conventional metal heat sink. The main disadvantage of the slot channel structure is that the surface injecting heat into the cooling medium is limited to the base plate area.

**Figure 8** shows a novel concept employing a metal inlay which is positioned directly below the power module base plate and provides a mini-channel structure for water flow. A rubber-ring between inlay and plastic heat sink ensures direct contact of the inlay fins and base plate metal surface. The gap between the inlay fins and the base plate is not filled with air ($\lambda_{AIR}=0.026\ W/(Km)$) and/or thermal grease but with water ($\lambda_{H2O}=0.630\ W/(Km)$) what results in a significant reduction of the thermal resistance. The heat is flowing from the base plate partly directly into the water, and partly into the fins what effectively increases the cooling surface and results in a significant reduction of the thermal resistance. In the following the inlay geometry will be optimized for minimum thermal resistance. The geometry of the inlay-channels will be characterized by

$$k = \frac{b_{MI}}{b/n} \quad . \tag{15}$$

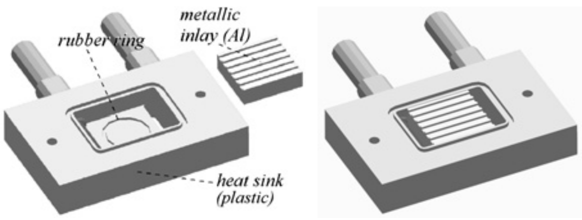


**(a)** **(b)**

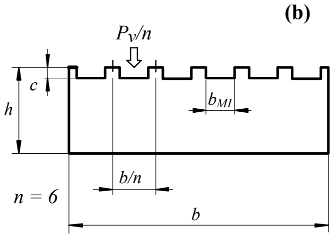


**(c)**

**Fig.8:** Novel metallic inlay concept **(a)** outside of the plastic heat sink and **(b)** embedded. **(c)** Geometry of metal inlay (*h=6mm*, *b=19.2mm*).

***Remark:*** The inlay-concept is advantageous only if the thermal resistance of the non-moving water layer $d_{interface}$ in the gap between base plate and inlay fins is smaller than the thermal resistance of the simple slot channel. If this condition is violated the thermal resistance of the proposed concept will always be higher in comparison with the slot channel scheme. **Figure 9** shows, that for the system under investigation (pump characteristic as given in (1), geometry of the power module base plate *3.4 x 2.5cm²*) the condition $R_{th,H2O}^{'} < R_{th,SlotChannel}^{'}$ is fulfilled. The thickness of the interface $d_{interface}$ is assumed to be about $1\mu m$ due to the surface roughness of base plate and inlay fins measured under the microscope.

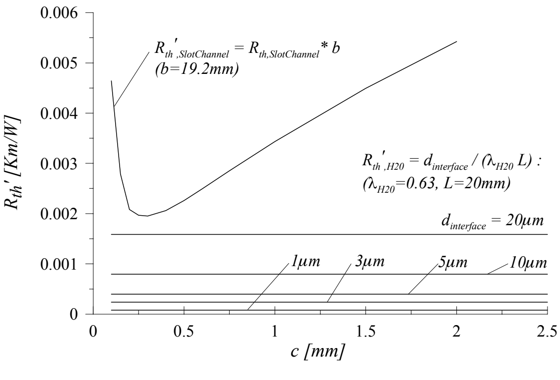


**Fig.9:** Comparison between normalized thermal resistance of the simple slot channel ($R_{th,SlotChannel}^{'}$) and normalized thermal resistance of an interface layer consisting of non-moving water ($R_{th,H2O}^{'}$) as given between base plate and fins of the metal inlay.

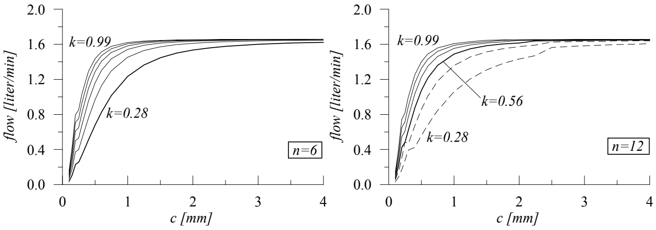


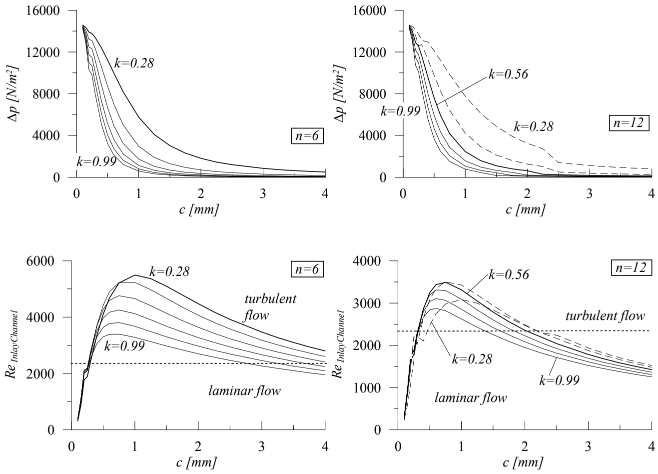


**Fig.10:** Water flow, pressure drop and Reynolds number indicating laminar or turbulent flow in dependency of the inlay geometry with *n=6* and *n=12*. Dashed curves indicate that the condition of easy manufacturing ($b_{MI}$ *>0.9mm*) is violated. Parameter of the family of curves is the channel ratio *k* = $b_{MI}/(b/n)$= *[0.28, 0.42, 0.56, 0.70, 0.84, 0.99]*. The dotted horizontal line marks the border between laminar and turbulent flow at $Re_{InlayChannel} = 2300$. For channel ratios $k = b_{MI}/(b/n)$ close to *1.0* (decreasing width of the fins) the cross section of the inlay ($n \cdot b_{MI}\, c$) becomes equal to the cross section of the slot channel ($b \cdot c$) but the pressure drop is different because of mechanical friction of the fluid along the fins which is independent from the width of the fins. Therefore, $Re_{InlayChannel}$ for *k=0.99* in Fig.10 is different for different channel-numbers *n* and is also different from $Re_{Channel}$ in Fig.3.

### *3.2 Calculation of Water Flow and Pressure Drop*

Defining the hydraulic diameter $d_h = 2b_{MI}\, c/(b_{MI} + c)$ for the geometry given in Fig.(5c) the water flow through the inlay channels creates a pressure drop across the heat sink which is given for laminar flow as ((3.221) in [3])

$$\Delta p_{Inlay,lam}(\dot{v}) = \frac{32\,\rho\,\nu\,L}{n(b_{MI}\,c)\,d_h^2}\ \dot{v} \tag{16}$$

with number of channels *n*. For turbulent flow the pressure drop is given as ((3.261) in [3])

$$\Delta p_{Inlay,turb}(\dot{v}) = \frac{L\,\frac{b_{MI}+c}{2b_{MI}\,c}\,\rho\,\frac{1}{2}\left(\frac{\dot{v}}{n(b_{MI}\,c)}\right)^2}{\left(0.79\cdot\ln\!\left(\frac{2\dot{v}}{n\,(b_{MI}+c)\nu}\right)-1.64\right)^2} \tag{17}$$

with the Reynolds number defined for this problem as (page 351 in [3])

$$\mathrm{Re}_{InlayChannel} = \frac{w_m \cdot d_h}{\nu} = \frac{2\dot{v}}{n(b_{MI}+c)\nu} \tag{18}$$

indicating laminar flow for $Re_{InlayChannel} < 2300$, and turbulent flow otherwise. Proceeding in analogy to section (2.2) water flow and pressure drop for certain geometries of the inlay channel structure can be calculated as shown in **Fig.10**. There, pump and cooling system are given by the measured characteristic (1).

### *3.3 Calculation of the Thermal Resistance of the Power Module Base Plate*

With the definition of the Reynolds number (18) the Nusselt number $Nu_{InlayChannel,lam}$ can be calculated for laminar flow ($Re_{InlayChannel} < 2300$) as ((3.250), (3.255) in [3])

$$Nu_{InlayChannel,lam} = \frac{3.657\left[\tanh\left(2.264X^{1/3} + 1.7X^{2/3}\right)\right]^{-1} + \frac{0.0499}{X}\tanh(X)}{\tanh\left[2.432\ \mathrm{Pr}^{1/6}\ X^{1/6}\right]} \qquad (19)$$

with $$X = \frac{L}{d_h\ \mathrm{Re}_{InlayChannel}\ \mathrm{Pr}}, \qquad (20)$$

and for turbulent flow ($Re_{InlayChannel}$ > *2300)* as ((3.260), (3.261) in [3])

$$Nu_{InlayChannel,turb} = \frac{\{8\cdot(0.79\cdot\ln(\mathrm{Re}_{InlayChannel}) - 1.64)^2)\}^{-1}(\mathrm{Re}_{InlayChannel} - 1000)\ \mathrm{Pr}}{1 + 12.7\sqrt{\{8\cdot(0.79\cdot\ln(\mathrm{Re}_{InlayChannel}) - 1.64)^2)\}^{-1}}\ (\mathrm{Pr}^{2/3} - 1)}\left[1 + \left(\frac{d_h}{L}\right)^{2/3}\right] \qquad (21)$$

In contrast to the theory of the water flow along a hot plate described by (6) and (7) in connection with the slot channel the determination of the heat transfer problem of the inlay concept (equations (19) - (21)) is based on the theoretical model of rectangular channels where all walls are heated. Under the assumption of a good thermal conductivity of the metallic inlay ($\lambda_{Al}=237\ W/(Km)$) this is valid in good approximation.

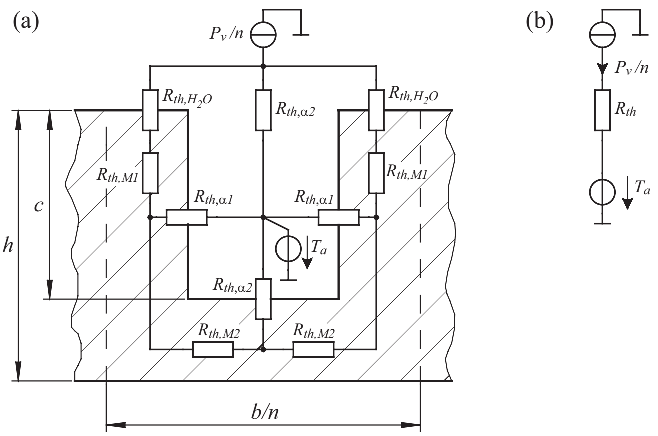


**Fig.11: (a)** Thermal network describing (stationary) heat conduction between power module base plate and the water (temperature $T_a=40°C$). The thermal power flow is direct ($R_{th,\alpha2}$) and via the metal inlay. The resistance values of the thermal equivalent circuit are given in (16). **(b)** The network can be transformed into a single resistance $R_{th}$ as defined in (23).

$$\alpha = Nu_{InlayChannel}\cdot\lambda_{H20}/d_h$$
$$R_{th,H20} = d_{interface}/(\lambda_{H20}\,L\,(b/n-b_{MI})/2)$$
$$R_{th,M1} = (c/2)/(\lambda_{Al}\,L\,(b/n-b_{MI})/2)$$
$$R_{th,M2} = R_{th,M1} + (b_{MI}/2)/(\lambda_{Al}\,L\,(h-c))$$
$$R_{th,\alpha1} = 1/(\alpha\,L\,c) \qquad R_{th,\alpha2} = 1/(\alpha\,L\,b_{MI}) \qquad (22)$$

$$R_{th} = R_{th}\,(d_{interface}, Nu_{InlayChannel}) =$$
$$= R_{th,\alpha2}\ ||\ [(½R_{th,H20} + ½R_{th,M1}) + (½R_{th,M2} + R_{th,\alpha2})\ ||\ (½R_{th,\alpha1})] \qquad (23)$$

The network of thermal resistances in **Fig.11** describes the heat transfer from the power module base plate into the water for one channel. There, $R_{th,H20}$ is the thermal resistance of the contact area between the fins and the base plate. For calculating the thermal resistance $R_{th,H20}$ we assume a metallic surface roughness of $0.8\mu m$ … $1.6\mu m$ (measured with the microscope), neglect small areas where both metal surfaces are in direct contact, and assume that the gap between both surfaces is entirely filled with water. This contact area will be modeled as a layer of non-moving water with a thickness of $d_{interface}=1.0\mu m$. The resulting thermal resistance $R_{th,H20}$ can be calculated according to (22).

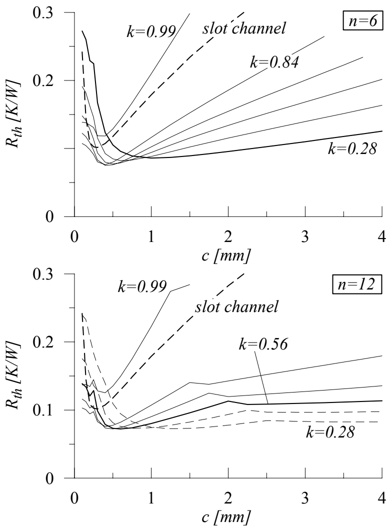


**Fig.12:** Thermal resistance between power module base plate and water dependent on the height *c* of the channel (cf. Fig.8(c)) with channel ratio $k= b_{MI}/(b/n)$ for $n=6$ and $n=12$. The curves are given for channel ratios $k= b_{MI}/(b/n)= [0.28, 0.42, 0.56, 0.70, 0.84, 0.99]$.

In analogy to section (2.3) the thermal resistance can be calculated from (16) - (23) dependent on the geometry of the inlay structure (**Fig.8**). Concerning heat flow for $k=0.99$ the influence of the fins is negligible and the inlay geometry is equal to the slot channel geometry. The curve of the slot channel (Fig.4(a)) is shown in both diagrams as dotted line and is very close to the inlay channel curve of $k=0.99$. As the slot channel and metal inlay considerations are based on different theories of heat transfer (see previous section) this result shows the good consistency of all analytic equations describing the heat transfer problems in this paper. But, as discussed in the text of Fig.10, these two geometries are not equivalent concerning pressure drop and Reynolds number. Since the Nusselt number is dependent on the Reynolds number ((7), (19) - (21)) small differences between the two curves especially at higher values of *c* can be explained. For $n=12$ the geometries that are difficult to manufacture (condition for easy manufacturing: $k>0.55 \rightarrow b_{MI} >0.9mm$) are shown by dashed lines.

### *3.4 Experimental Results*

The calculations (16)-(23) resulting in the characteristics of Fig.12 are performed neglecting the influence of the internal pipe structure of the heat sink. Since this pipe structure is unchanged, equations (11) and (section 2.4.2) can be employed using the same parameter values $x_a$, $x_b$ as given in section (2.4). The channel cross section $A_{q,SlotChannel}$ in (11) has to be replaced with the inlay channel cross section $A_{q,InlayChannel}$ that can be directly expressed in channel height *c* as

$$A_{q,InlayChannel} = n\cdot b_{MI}\cdot c = k\cdot b\cdot c\ . \qquad (24)$$

Experiments have been performed in analogy to the description in section (2.5) with different inlay geometries for ($n=6$ / $k=0.31$ / $c=0.2mm$, $c=1.25mm$, $c=2mm$, $c=3mm$)

and (*n=12 / k=0.63 / c=0.2mm, c=1.25mm, c=2mm, c=3mm*). The measurement results presented in **Fig.13** show a close match with the theory and the analytical calculations.

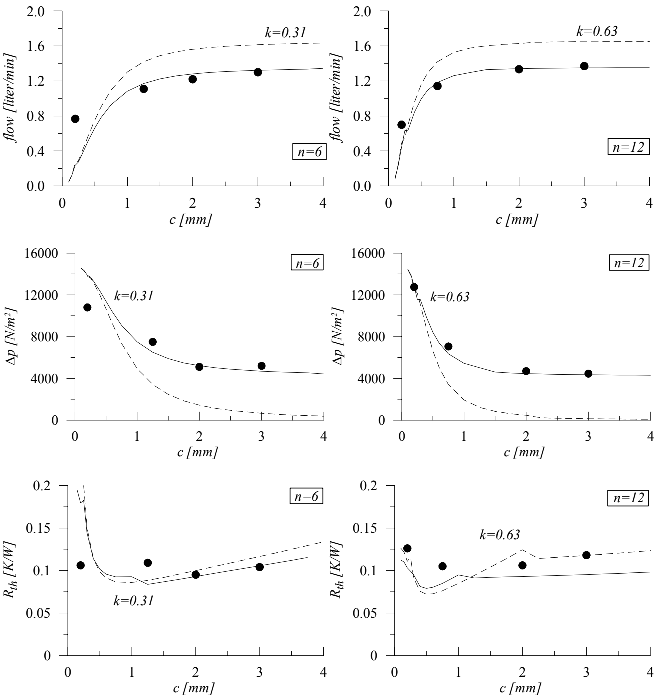

**Fig.13:** Neglecting the influence of the pipe structure inside the heat sink results in the characteristics shown in dashed lines (already shown in Fig.10 and Fig.12). Performing the calculations as described in section (2.4) gives the curves shown by solid lines. The black dots are results of experimental measurements. For $n=6$ inlay-channels we manufactured a structure $k=b_{MI}/(b/n)=1.0mm/(19.2mm/6)=0.31$ and for $n=12$ we manufactured a heat sink structure $k=b_{MI}/(b/n)=1.0mm/(19.2mm/12)=0.63$.

## IV. COOLING MULTI-CHIP MODULES

All theory presented is based on the assumption of equal distribution of the thermal power flow through the base plate area. Also the experiments have been performed under this assumption by employing a copper block acting as a very efficient heat spreader and guiding the heat from the heating resistors directly to the base plate. The $R_{th}$-values presented in Fig.7 and Fig.13 must be interpreted under this assumption. If a small chip with area $A_{CHIP}<A_{BasePlate}$ is positioned inside the power module, heat spreading will increase the cross sectional area available for heat flow and reduce the thermal resistance. Employing the inlay concept the total thermal resistance will be reduced because the metallic inlay itself will contribute to heat spreading. If the power module's base plate is made of a thick copper plate (*2…3mm*) the copper plate will perform the heat spreading and the slot channel scheme might be sufficient.

## V. CONCLUSION

This paper presents a method how to calculate the thermal resistance between power module base plate and ambient for water cooling with purely analytical equations. All equations shown in this paper have been put into a *Mathematica* [9] script to immediately calculate thermal resistance values for various geometries. Doing numerical simulations instead would be extremely time-consuming and not practical, therefore. Experimental results have shown the high accuracy of the theory.

Considering the characteristic of the pump is essential to find the optimum geometry for minimizing the thermal resistance. A simple slot channel schema shows very good results. Employing a novel inlay scheme as proposed in the paper will reduce the thermal resistance and will do the heat spreading in case of a multi-chip power module which will further reduce the thermal resistance. According research is being performed.

The pump discussed in the paper accomplishes a pressure of about *80mbar* and a water flow of *1.2liter/min* which gives for the optimized inlay channel scheme a thermal resistance $R_{th,BasePlate\text{-}ambient}$ of less than *0.85K/W* per $cm^2$ (*0.1K/W* for a *2.5cmx3.4cm* base plate).

## REFERENCES


[1] **Kolar, J.W. and Zach, F.C.:** *A Novel Three-Phase Utility Interface Minimizing Line Current Harmonics of High-Power Telecommunications Rectifier Modules.* Record of the 16th IEEE International Telecommunications Energy Conference, Vancouver, Canada, Oct. 30 - Nov. 3, pp. 367-374 (1994).

[2.1] **Spurk, J.H.:** *Strömungslehre – Einführung in die Theorie der Strömungen* (in German). ISBN 3-540-61308-0, 4th edition, Springer-Verlag (1996).

[3] **Baehr, H.D. and Stephan, K.:** *Wärme- und Stoffübertragung* (in German). ISBN 3-540-64458-X, 3rd edition, Springer-Verlag (1998).

[4] **Tuckermann, D.B. and Pease, R.F.W.:** *High-Performance Heat Sinking for VLSI.* IEEE Electronics Device Letter, Vol. EDL-2, pp. 126 – 129, May (1981).

[4.2] **Beitz, W. and Grote, K.-H.:** *Dubbel – Taschenbuch für den Maschinenbau* (in German). ISBN 3-540-67777-1, 20th edition, Springer-Verlag (2001).

[5] **Brignoni, L.A., and Garimella, S.V.:** *Experimental Optimization of Confined Air Jet Impingement on a Pin Fin Heat Sink.* IEEE Transactions on Components and Packaging Technology, Vol. 22, No. 3, pp. 399 – 404, Sept. (1999).

[6] **Drofenik, U., and Kolar, J.W.:** *Thermal Analysis of a Multi-Chip Si/SiC-Power Module for Realization of a Bridge Leg of a 10kW Vienna Rectifier.* Proceedings of the 25th IEEE International Telecommunications Energy Conference, Yokohama, Japan, Oct. 19 - 23, pp. 826 - 833 (2003).

[7] **Murakami, Y., and Mikic, B.B.:** *Parametric Optimization of Multichanneled Heat Sinks for VLSI Chip Cooling.* IEEE Transactions on Components and Packaging Technology, Vol. 24, No. 1, pp. 2 – 9, March (2001).

[8] **Mudawar, I.:** *Assesment of High-Heat-Flux Thermal Management Schemes.* IEEE Transactions on Components and Packaging Technology, Vol. 24, No. 1, pp. 122 – 141, March (2001).

[9] *Mathematica*: http://www.wolfram.com/